Published online 29 July 2022

NAR Cancer, 2022, Vol. 4, No. 3 **1**
https://doi.org/10.1093/narcan/zcac024

KAP1 is a new non-genetic vulnerability of malignant pleural mesothelioma (MPM)

Eugenia Lorenzini[1,2], Federica Torricelli[1], Raffaella Zamponi[1], Benedetta Donati[1], Veronica Manicardi[1,3], Elisabetta Sauta[1,4], Italo Faria do Valle[5], Francesca Reggiani[1], Mila Gugnoni[1], Gloria Manzotti[1], Valentina Fragliasso[1], Emanuele Vitale[1,3], Simonetta Piana[6], Valentina Sancisi[1] and Alessia Ciarrocchi[1,*]

[1]Laboratory of Translational Research, Azienda USL-IRCCS di Reggio Emilia, 42123 Reggio Emilia, Italy, [2]Cellular and Molecular Biology PhD Program, University of Bologna, 40126 Bologna, Italy, [3]Clinical and Experimental Medicine PhD Program, University of Modena and Reggio Emilia, 41121 Modena, Italy, [4]Department of Electrical, Computer and Biomedical Engineering, University of Pavi,, 27100 Pavia, Italy., [5]Department of Physics, Center for Complex Network Research, Northeastern University, Boston, MA 02115, USA. and [6]Pathology Unit, Azienda USL-IRCCS di Reggio Emilia, 42123 Reggio Emilia, Italy

Received February 22, 2022; Revised June 29, 2022; Editorial Decision July 08, 2022; Accepted July 16, 2022

ABSTRACT

Malignant pleural mesothelioma (MPM) is a rare and incurable cancer, which incidence is increasing in many countries. MPM escapes the classical genetic model of cancer evolution, lacking a distinctive genetic fingerprint. Omics profiling revealed extensive heterogeneity failing to identify major vulnerabilities and restraining development of MPM-oriented therapies. Here, we performed a multilayered analysis based on a functional genome-wide CRISPR/Cas9 screening integrated with patients molecular and clinical data, to identify new non-genetic vulnerabilities of MPM. We identified a core of 18 functionally-related genes as essential for MPM cells. The chromatin reader KAP1 emerged as a dependency of MPM. We showed that KAP1 supports cell growth by orchestrating the expression of a G2/M-specific program, ensuring mitosis correct execution. Targeting KAP1 transcriptional function, by using CDK9 inhibitors resulted in a dramatic loss of MPM cells viability and shutdown of the KAP1-mediated program. Validation analysis on two independent MPM-patients sets, including a consecutive, retrospective cohort of 97 MPM, confirmed KAP1 as new non-genetic dependency of MPM and proved the association of its dependent gene program with reduced patients' survival probability. Overall these data: provided new insights into the biology of MPM delineating KAP1 and its target genes as building blocks of its clinical aggressiveness.

GRAPHICAL ABSTRACT

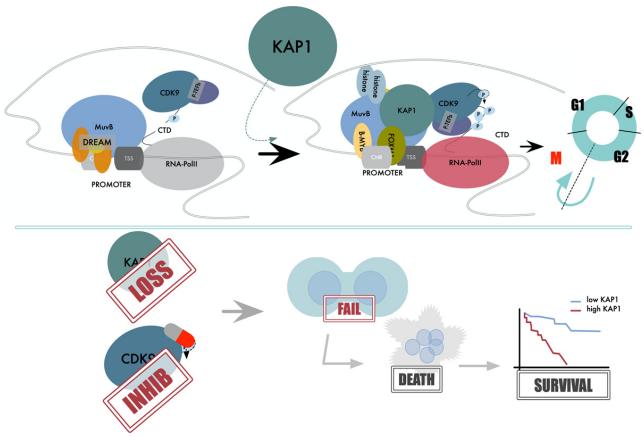

INTRODUCTION

Malignant Pleural Mesothelioma (MPM) is a rare but highly aggressive cancer arising from the mesothelial cells lining the pleura (1,2). It is characterized by high mortality rate and dismal prognosis due to the limited treatment options currently available. MPM is associated with chronic asbestos exposure. Its widespread use in the 20th century and the long latency makes MPM a current clinical challenge (1–4).

Molecular bases of this disease remain unknown, representing the most relevant limitation to the development of MPM targeting strategies (5). Insights into the genetic landscape of this tumor revealed a quite low mutational burden and few pathologically relevant mutations. Furthermore, no specific MPM genetic alterations can be attributed

*To whom correspondence should be addressed. Tel: +39 0522295668; Email: Alessia.Ciarrocchi@ausl.re.it

to the direct action of asbestos (6–10). Instead, increasing evidence points to an epigenome-centered effect of asbestos on the genesis and progression of MPM (7,8,11,12). Chromatin plasticity is at the basis of many fundamental processes including transcription, chromosome condensation and DNA damage repair (DDR). All these processes are boosted in cancer to sustain the massive proliferation of tumor cells. For this reason, epigenetic readers that works as multi-task units to coordinate DNA-based processes are emerging as essential factors for cancer maintenance and survival (13).

KRAB-associated protein 1 (KAP1), also known as TRIM28, is a large multi-domain protein with highly versatile chromatin associated functions. By coordinating the assembly of large multiprotein complexes on DNA, KAP1 modifies chromatin local structure affecting both transcription and DNA repair (14,15). In controlling gene expression, KAP1 can act either as repressor or as activator of specific genes. By recruiting components of the Nucleosome Remodeling Deacetylase complex (NuRD) and the histone methyl transferase SETDB1, KAP1 primes chromatin condensation and gene repression (16,17). On the other site, KAP1 promotes efficient but selective gene expression, by fostering recruitment on site of both pathway-specific Transcription Factors (TFs) and CDK9 to induce TF-mediated CDK9-dependent RNA-PolII activation, therefore coupling transcription initiation and elongation (18,19). For its centrality as reader of genome function, KAP1 and its functional network are currently regarded as attractive potential targets for new anticancer drugs.

In this work, we performed a genome-wide CRISPR/Cas9 knockout screening (20) integrated with the analysis of clinical and molecular data from the TCGA MPM-dataset (MESO-TCGA) (7), with the intent of providing new insights into the pathobiology of MPM and of identifying genes essential for MPM growth and survival. KAP1 emerged as a non-genetic vulnerability of MPM and negative prognostic factor in patients. Mechanistically, KAP1 is required for the cycling and synchronous expression of G2/M genes therefore participating to the timing of mitosis execution and cell cycle progression. Treatment with CDK9 inhibitors abolished this cooperation leading to the deep inhibition of KAP1 transcriptional program and to massive MPM cells death. Finally, validation analysis in an independent cohort of MPM patients confirmed KAP1 and its target genes as associated with reduced survival probability and indicate these genes as novel negative prognostic markers in MPM.

MATERIALS AND METHODS

Cell culture

MSTO-211H cell line was obtained from Istituto Europeo di Oncologia (IEO, Milan, Italy). NCI-H2052, HEK293T, Toledo and NK-92 cell lines were obtained from ATCC (LGC Standards, Sesto San Giovanni, Italy). MSTO-211H, NCI-H2052, Toledo and HEK293T cell lines were cultured in RPMI medium added with 10% fetal bovine serum (FBS) and 1% penicillin–streptomycin. NK-92 were cultured in MEM α, no nucleosides, complemented as reported in ATCC guidelines. All cell lines were grown at 37°C/5% CO_2. Cell lines were routinely tested for Mycoplasma contamination and authenticated by SNP profiling at Multiplexion GmbH (Heidelberg, Germany).

CRISPR/Cas9 genome-wide screening and target selection

Genome-wide screening was performed as previously described (21,22) using semi-library A of the Human GeCKOv2 CRISPR knockout pooled library in lentiGuide-Puro plasmid (Addgene #1000000049) in two separate replicates. 180×10^6 cells with a multiplicity of infection (MOI) of 0.3, aiming at 600× coverage were infected. After puromycin selection, 120 million cells were harvested to sequence T0 time point. The remaining cells were cultured and 120 million cells were collected at 16 and 23 days after selection starting. Libraries preparation, sequencing and bioinformatic analysis were performed as already described (21,22).

Only genes consistently detected in both experiments (A1 and A2) and at both time-points (T16, T23) were considered. We excluded miRNAs (163 for essentials and 10 for suppressors) and genes that are essential for cell viability in all cell lines (608) as listed in the 'Achilles_common_essential' list from the DEPMAP database. The 'DEPMAP' database (23) was interrogated to further validate our analysis. Only genes that were coherent in at least six of the seven MPM cell lines available in this database were considered as validated. 51% and 26% of essential and suppressor genes were confirmed respectively by this approach, obtaining a final list of 233 MPM essential genes and 45 MPM suppressor genes.

TCGA data analysis

Survival data and gene expression profile on MPM patients were obtained from The Cancer Genome Atlas (TCGA) dataset using the R TCGA biolinks package to download and analyze RNAseq data (workflow.type 'HTSeq - FPKM'). Gene expression values were correlated using R Corrplot package. For survival analysis, performed with R Survival package, patients were dichotomized on the basis of first and fourth quartile of genes expression. Genetic variations in MPM were selected among the most altered genes in MPM using cBioPortal (http://www.cbioportal.org) based on TCGA datasets. Differential expression analysis for the 18 core genes was conducted according to mutational status. Significant associations were evaluated by Kruskall–Wallis test.

Knockout cell lines generation and competition assays

Two sgRNAs for each target gene were selected from the GeCKOv2 library and cloned into the pLKO5.sgRNA.EFS.GFP plasmid (gift from Benjamin Ebert; Addgene plasmid #57822) into BsmBI cloning site. sgRNAs sequences are listed in Supplementary Table 4. 500 000 MSTO-211H/Cas9 cells were seeded in a six-well plate and the day after they have been infected as described in Supplementary Information. Knockout efficiency was assessed by T7 endonuclease I cleavage assay (ALT-R Kit, Integrated DNA Technologies, Skokie, Illinois, USA)

following manufacturer instructions. Infection efficiency was assessed by GFP detection with a FACS Canto II Flow Cytometer. Cells showing <90% GFP positive cells were sorted using a FACS Melody (BD Biosciences). Protein and gene expression analysis were performed both at 5 and 7 days after infection.

For competition assays, cells were infected with a MOI of 0.6–0,7 and grown for 15 days to assess the competition between the two populations of infected (GFP+) and non-infected (GFP–) cells. The percentage of GFP+ (infected) cells was recorded with a FACS-Canto II Flow Cytometer at the specified time points and normalized on T0. T0 was collected 4 days after infection. A non-targeting sgRNA was used as a negative control, while two sgRNAs targeting ATP2A2 (common essential gene) were used as positive controls.

*siRNA Transfections qRT-PCR and Western Blot analysis w*ere conducted as previously described (24–26). Supplementary Tables 5-7 for primers, antibodies and siRNA sequences used.

Proliferation and colony forming assays

MSTO-211H and NCI-H2052 cells were seeded 24h post transfection at a density of 2500 cells/well in a 96-well plate. Images were recorded every 6 h for 96 h by the Incucyte® S3 Live-Cell Analysis System (Sartorius).

For colony forming assays, cells were seeded in 10 cm culture dishes at density of 10 000 cells (MSTO-211H) or 2500 cells (NCI-H2052) per dish and grown for 10 days. Colonies were stained with crystal violet solution (0.5% in H_2O) and counted using the ImageJ software.

Cell cycle analysis and apoptosis

Cell cycle analysis were performed in MSTO-211H/Cas9 cells infected with either a negative control sgRNA (NT1) or a sgRNA targeting KAP1 (KAP1-sg.1), 4 days after infection. Cells were analyzed by Nicoletti solution staining (27) with a FACS Canto II Flow Cytometer (BD Biosciences). For apoptosis, cells were harvested in Annexin Buffer (BD Biosciences), stained with PE Annexin V and 7-Amino-Actinomycin (7AAD) (BD Biosciences) and analyzed using a FACS Canto II Flow Cytometer (BD Biosciences).

For cell cycle analysis after CDKi treatment, 2×10^5 MSTO-211H cells and 1.5×10^5 NCI-H2052 cells were seeded in Matrigel-coated 12-well plates (Corning). 16h later, CDK9i was added and after 12 h cells were synchronized and processed as described above.

Immunofluorescence

Immunofluorescence was conducted as previously described (25,26).

RNA-Seq and bioinformatics analysis

RNA was collected 7 days after infection of MSTO-211H/Cas9 cells using two sgRNAs targeting KAP1 and a non-targeting sgRNA as a control, in two independent experiments. RNA was assessed by Bioanalyzer RNA 6000 nano kit (Agilent Technologies, Santa Clara, California, USA). Libraries were obtained from 500 ng of total RNA using Illumina TruSeq Stranded Total RNA and sequenced using Illumina NextSeq high-output cartridge (2×75). Sequencing quality was assessed using the FastQC v0.11.8 software (www.bioinformatics.babraham.ac.uk/projects/fastqc/). Raw sequences were then aligned to the human reference transcriptome (GRCh38, Gencode release 30) using STAR version 2.7 (28) and gene abundances were estimated with RSEM algorithm (v1.3.1) (29). Differential expression analysis was performed using DESeq2 R package (30), considering a False Discovery Rate (FDR) of 10% and excluding genes with low read counts. Only genes coherently de-regulated by both sgRNAs were considered. Significant deregulated genes underwent to enrichment analysis, performed on Gene Ontology biological processes, KEGG and Reactome pathways databases via enrichR package (31) and ClueGO (32) via Cytoscape for graphical purpose, using a significance threshold of 0.05 on *P*-value corrected for multiple testing using Benjamini–Hochberg method. Data are available at ArrayExpress (E-MTAB-10942).

Patients selection and nanostring analysis

A retrospective cohort of 97 MPM consecutive patients was retrieved from the Pathology Unit of our Institution between 2010 and 2021. Inclusion criteria were availability of Formalin Fixed Paraffin Embedded (FFPE) tumor tissues and follow up information. The main endpoint of this analysis was the association between gene expression profiles in tumor specimens and patients' survival. The median overall survival was 15 months (IQR 9–25). Histological sections of all samples were revised by two different pathologists. Project was approved by local ethic committees.

Total RNA was extracted by Maxwell® RSC RNA FFPE kit (Promega) starting from five slides of 5 μm FFPE tissue. RNA quantity and quality were assessed by NanoDrop 2000 (Thermo Fisher Scientific). Eighty-six samples reached the RNA quality standard required ($A_{260}/A_{280} \geq 1.7$ and $A_{260}/A_{230} \geq 1.8$) Clinical Features of these patients are reported in Table 1. Gene expression in these samples was evaluated by NanoString using a custom panel called MPM_C9073 (NanoString Technologies) following manufacturers' protocol. This panel was specifically designed on this purpose, including 70 genes among which KAP1, 36 genes identified as KAP1's target, 17 genes considered essential for MPM survival and 20 housekeeping genes.

Analysis of detected gene counts was performed by nSolver Analysis Software 4.0 (NanoString Technologies). For samples that passed imaging quality controls, raw genes counts were normalized on technical controls and three housekeeping genes (AMMECR1L, ERCC3, ZNF346) among the ones included in the panel as previously described (33). The complete matrix of normalized counts is available at GEO repository (accession number: GSE183088). Gene expression values of KAP1 and its target genes were correlated using Spearman method.

Then patients were stratified according to OS and Fold Changes (FCs) were calculated as ratio between the expression profile of short- survival samples (first quartile: 20/86)

Table 1. Clinical Features of the MPM cohort used in the validation analysis

	Total ($N = 86$)
Sex	
F	21 (24.4%)
M	65 (75.6%)
Age	
≤65	25 (29%)
>65	61 (71%)
Histology	
Biphasic	36 (41.8%)
Epithelioid	44 (51.2%)
Sarcomatoid	6 (7%)
Status	
Alive	11 (12.8%)
Deceased	75 (87.2%)
Stage	
1	45 (52.3%)
2	6 (7%)
3	10 (11.6%)
4	23 (26.8%)
Missing	2 (2.3%)
Type of surgery	
Biopsy	43 (50%)
Pleurectomy	43 (50%)
Asbestos exposure	
Domestic	8 (9.3%)
Professional	67 (77.9%)
NO	7 (8.1%)
Missing	4 (4.7%)
Smoking	
No	27 (31.4%)
Yes	28 (32.6%)
Missing	31 (36%)
Chemotherapy treatment	
No	21 (24.4%)
Yes	63 (73.3%)
Missing	2 (2.3%)
Response to chemotherapy	
No	34 (39.5%)
Yes	22 (25.6%)
Missing	30 (34.9%)

and long- survival samples (fourth quartile: 22/86). For each comparison *P*-value (as two-tailed Student's *t* test) and false discovery rate (FDR) obtained by Benjamini–Hochberg method, were calculated. For survival analysis, patients were dichotomized on the basis of first and fourth quartile of genes expression, and hazard ratio was calculated by Cox Model corrected for chemotherapy treatment. Bioinformatic analyses on GEP was conducted by R Software v4.0.3 using the following R packages: corrplot, ggplot2, ggbiplot (function prcomp), forestplot and survival.

CDKs inhibitors

Cells were seeded at 2500 cells/well in 96-well plates and treated with AT7519 and AZD4573 (Selleckchem, Munich, Germany) or DMSO. Both drugs were resuspended in DMSO (Sigma-Aldrich, St. Louis, Missouri, USA).

Statistical analysis

Statistical analysis was performed using GraphPad Prism Software (GraphPad Software, San Diego, California, USA). Statistical significance was determined using the student's *t* test. Each experiment was performed 2–6 times.

Additional Materials and methods are in the Supplementary Information section.

RESULTS

Integration of genome-wide CRISPR/Cas9 screening and patients data identified a chromatin-associated functional core of 18 MPM essential genes

To search for new vulnerabilities in MPM we performed a CRISPR/Cas9-based genome-wide knockout screening to identify genes essential for MPM. We infected the MPM cell line MSTO-211H cells, previously engineered to express Cas9 (Supplementary Figure 1A, B), with the GeCKOv2 library, targeting over 19 000 genes in the human genome (20). Cells were harvested at 16 and 23 days after selection. Library composition was assessed by next-generation sequencing (NGS) and single-guide RNAs (sgRNAs) frequencies were compared to day 0, to assess sgRNAs that were depleted and/or enriched over cell growth (Figure 1A–D). Our analysis was focused on sgRNAs depleted overtime, targeting genes that are essential for MPM growth and survival (essential genes). 1228 essential genes were consistently identified at both time points (Figure 1E). After exclusion of miRNAs and common essential genes (defined as essential genes for many if not all cell types), 457 MPM essential genes were identified. To validate these genes, we used the Cancer Dependency Map Project (DEPMAP) (23) that systematically identifies essential genes across over 500 cancer cell lines using either RNAi or CRISPR/Cas9 genome-scale genetic perturbation. Data from CRISPR/Cas9-screening were available for seven MPM cell lines including MSTO-211H. Over 51% (n = 233) of the identified genes were confirmed by this approach, supporting the validity of our analysis and underlining homogeneity in survival mechanisms across MPM cell lines (Figure 1D, E). GO analysis showed that these genes largely converged on cell cycle and chromatin and chromosomal organization (Figure 1F). A representative set of these genes was confirmed as essential in an independent experiment using a competition assay (Figure 1G).

To further refine this list and select clinical meaningful candidates, the expression of each of the 233 MPM essential genes identified was correlated with patients' survival probability using the MPM-dataset available in the TCGA repository ($n = 87$). The expression of 51 genes (22%) correlated with reduced survival probability of MPM patients ($P < 0.05$), among which 18 showed the strongest association ($q < 0.1$) (Supplementary Table 1). Coherently with the data obtained from the screening, >80% of these genes ($n = 15$) were involved in chromatin function and cell cycle regulation. Survival curves for these patients based on gene expression are shown in Figure 2A. The epigenetic reader KAP1 showed the most dramatic effect in terms of patients' survival, among the 18 genes identified. Low-KAP1 patients have a median survival of 43 months whereas high-KAP1 patients have a 11-month median survival (OR 6.3) (Figure 2A). Protein-protein network analysis showed that the 18 genes were all functionally interconnected (Figure 2B) and that their expression was positively correlated in patients through the TCGA MPM patients' cohort (Figure 2C, Supplementary Figure 2A, B).

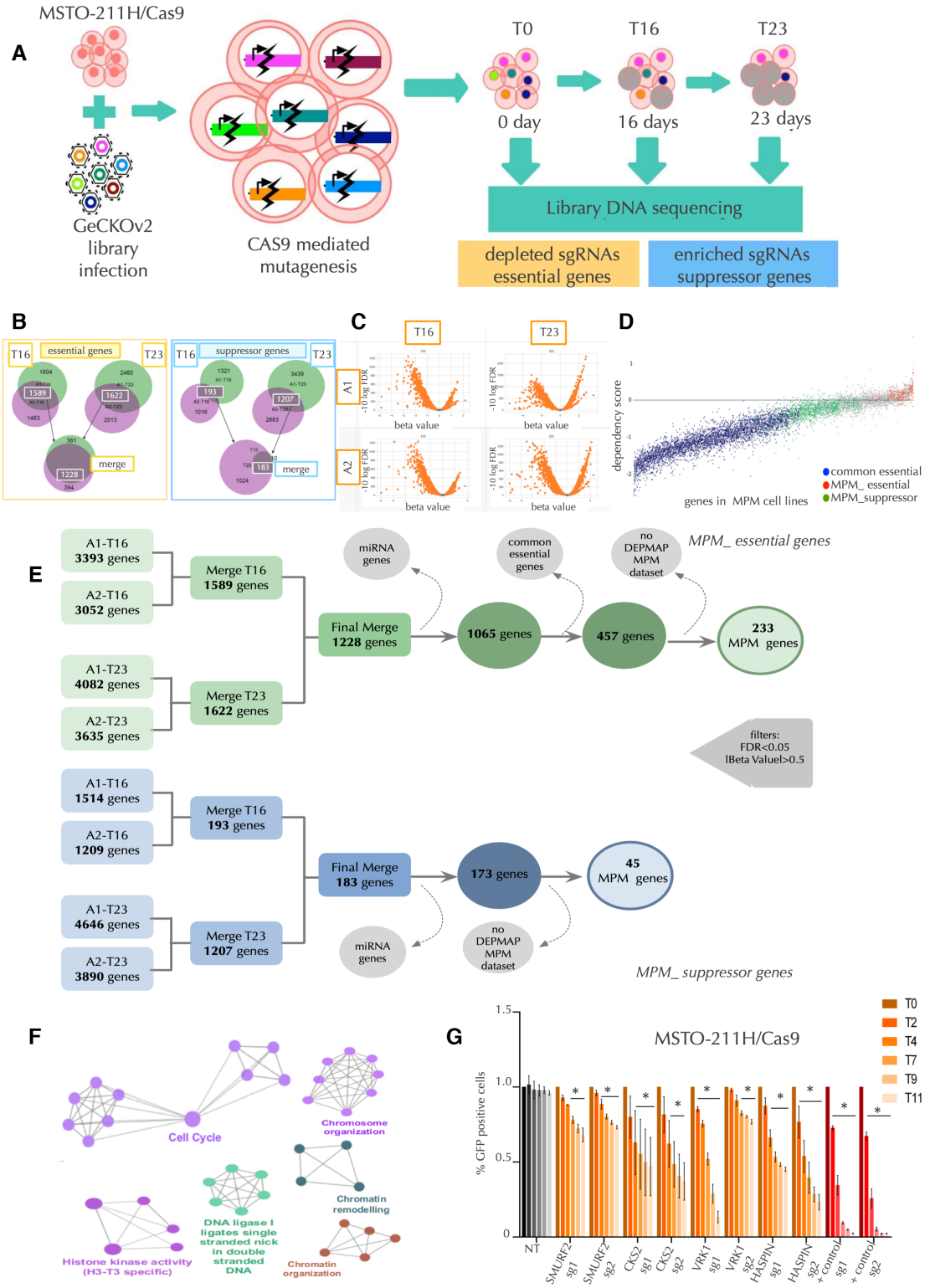

Figure 1. Genome-wide CRISPR-Cas9 screening in MSTO-211H cells. (**A**) Graphic overview of the genome-wide CRISPR/Cas9 screening performed in MSTO-211H cells; time points are relative to the start of the selection. (**B**) Venn diagrams reporting the number of genes identified in the two replicates at each time point and final merge for both essential (left) and suppressor (right) genes. (**C**) Volcano plots showing beta value and FDR adjusted *P*-value distributions at both time points and in each bio-replicate. (**D**) Graphic representation of the distribution of common essential, MPM essential and MPM suppressor genes in seven MPM cell lines according to DEPMAP database, ordered for dependency score. (**E**) Schematic representation of the flowchart that we adopted to analyze the screening results. (**F**) Network representation of the most significant enriched pathways for the 233 MPM essential genes. (**G**) Validation assay of the effect of the reported MPM essential genes using a competition assay. For each time point the ratio between GFP-positive (infected) and GFP-negative (uninfected) cells has been calculated and normalized on T0. Statistical significance has been calculated comparing the normalized ratio for each sample to T0. Data are mean ± SEM; $*P < 0.05$; $N = 2$.

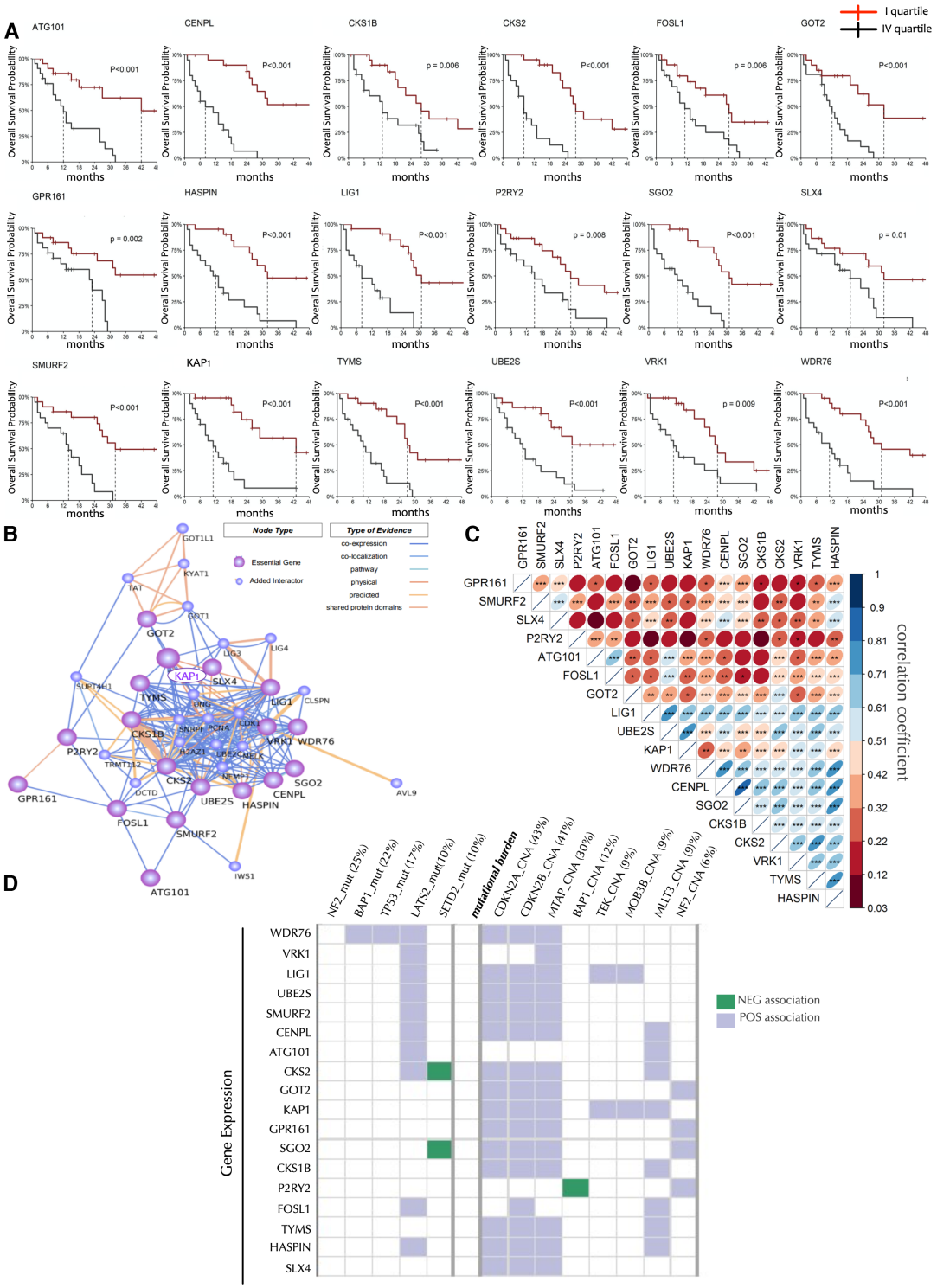

Figure 2. The genome-wide CRISPR-Cas9 screening identifies chromatin organization as key node for MPM progression. (**A**) Kaplan–Meier plots showing correlation of the 18 epigenetic readers with MPM patients survival based on TCGA data; ($N = 87$). Patients were divided in quartiles of gene expression and compared between first (red) and fourth (black) quartiles. (**B**) Protein–protein interaction network of the 18 epigenetic readers essential for MPM survival and added interactors by STRING (v11). The type of evidence linked to each edge is represented by a color scale. (**C**) Expression correlation matrix (Spearman test) within the 18 chromatin readers based on TCGA MPM data; $^{*}P < 0.05$, $^{**}P < 0.01$, $^{***}P < 0.001$. (**D**) Association among the expressions of the 18 chromatin readers and MPM most relevant mutations and mutational burden according to TCGA data. MPM samples were dichotomized based on the presence of mutations. Differential analysis was conducted to establish whether the expression of the 18 MPM essential epigenetic readers showed a significantly different distribution in the mutated vs non-mutated group. POS and NEG association mean respectively higher or lower gene expression (on Y axis) in presence of mutations (on X axis). Association was established by Kruskal test adjusted for Benjamini–Hochberg. Results were considered significant for $P_{\text{adjusted}} < 0.05$. Percentage of mutated patients is reported following the gene name. Genes showing CNA or mutations in less than 5 patients were not considered.

Moreover, analysis of association of their expression with MPM genetic alterations showed that, with the exception of ATG101 and P2Ry2, these genes were positively associated with copy number alterations in the cell cycle inhibitors CDKN2A, CDKN2B and methylthioadenosine phosphorylase (MTAP) which are often co-deleted together in cancer (34) (Figure 2D).

A subset of these genes (WDR76, VRK1, LIG1, UBE2S, SMURF2, CENPL, ATG101, FOSL1, HASPIN and CKS2) showed a positive association with LATS2 mutation. Altogether these data, besides confirming the validity of our analysis, indicate that the 18-genes identified in our screening may represent an essential functional core in MPM.

Loss of KAP1 impairs MPM cells proliferation and survival

We focused our analysis on KAP1 (also known as TRIM28), taken into consideration the profound effect on patients' survival and its reported role in genome function (14). Based on our analysis, KAP1 expression positively correlates with CDKN2A/B (Figure 2D).

Coherently, patients with loss of CDKN2A/B presented a significantly higher expression of KAP1 (Supplementary Figure 3A–D). To get deep on this, we performed an overall survival (OS) analysis evaluating the combined effect of KAP1 expression and CDKN2A deletion on MPM patients. Since CDKN2A and CDKN2B are co-deleted in the majority of patients (Supplementary Figure 3E), we took into consideration the CNA status of CDKN2A only. Noticeably, we observed that CDKN2A deletion had a negative effect on OS only on KAP1 low expressing patients, while the presence of this deletion did not affect the OS of high-KAP1 expressing patients (green and blue), suggesting that the expression of KAP1 has an important value in defining clinical aggressiveness of MPM (Supplementary Figure 3F).

Using the DEPMAP data, we searched for genetic alterations that correlate with KAP1 dependency. No significant association was defined (Supplementary Figure 4A–C). We also employed the TCGA transcriptional dataset to investigate the gene expression program correlating with KAP1 expression in this context. Noticeably, we observed that genes positively correlated with KAP1 were involved primarily in mitosis regulation (Supplementary Figure 4D). Competition assay in MSTO-211H/Cas9 cells confirmed that loss of KAP1 confers a significant growth disadvantage to MPM cells (Supplementary Figure 5A, B). Furthermore, silencing of KAP1 by siRNA in MSTO-211H and NCI-H2052 MPM cell lines resulted in a significant reduction of cell proliferation (Figure 3A. B, Supplementary Figure 5C, D), and a dramatic loss of colony forming ability (Figure 3C-D), confirming the requirement of KAP1 for proficient expansion of MPM cells. These results were confirmed also in the MSTO-211H/Cas9 cells transduced with a sgRNA targeting KAP1 (Supplementary Figure 5E). Cell cycle analysis in MSTO-211H/Cas9 cells showed that KAP1 KO induced a slight but consistent accumulation of cells in the G2/M phase (Figure 3E). Furthermore, KAP1 KD caused in both cell models a significant increase of apoptosis as demonstrated by Annexin V/7AAD staining and increased expression of the pre-apoptotic protein BAX (Figure 3F–I).

KAP1 controls the expression of the mitotic gene program and is required for mitosis execution

To get deep into KAP1 biological function in MPM, we performed RNA-sequencing in MSTO-211H/Cas9 cells upon KAP1 KO, using two independent sgRNAs. Comparison with parental cells identified 607 genes whose expression was significantly affected by loss of KAP1 (Figure 4A–C). 277 (45.6%) genes were significantly downregulated while 330 (54.4%) were upregulated, confirming the ability of KAP1 to work efficiently as either activator or repressor of gene expression (Supplementary Table 2). GO analysis showed that KAP1 KO upregulated genes were related to innate-immunity and in particular to IFN-mediate immune response, in accordance with published data that describe KAP1 as regulator of retroelements and their effect on viral mimicry (Supplementary Figure 6A) (35).

Noticeably, a significant fraction of downregulated genes (n = 90/277, 32.5% of the total) takes part in cell cycle. Among these, 83.3% of genes (n = 75/90) is specifically involved in mitosis, as further confirmed by GO analysis (Figure 4A, B). Coherently, major players of mitosis including AURKA, AURKB, BIRC5, INCENP, CDCA8, BMYB and FOXM1 were significantly downregulated in KAP1 KO cells as compared to control (Figure 4C). Noticeably, TYMS, UBE2S, CKS1B and VRK1, identified as part of the 18 genes essential core for MPM in our screening, (Figure 2A–C) were highlighted as KAP1 targets in this analysis.

qRT-PCR and western blot validation confirmed in both MSTO-211H and NCI-H2052 (Figure 4D–G) and in MSTO-211H/Cas9 cells (Supplementary Figure 6B, C) that loss of KAP1 profoundly impaired the expression of G2/M genes including: pCDK1 (the active form of the cyclin-dependent kinase 1 (CDK1) that ensures G2/M phase transition), AURKA and AURKB (cell cycle-regulated kinases involved, respectively, in microtubule stabilization at spindle pole organization and chromosomes alignment/segregation) and H3pSer10 (marker of chromosome condensation) (36).

Coherently, KAP1 KD MSTO-211H cells displayed throughout mitosis a wide range of dramatic defects in chromosome condensation, mitotic fuse organization and function and chromosome segregation, monopolar spindle with abnormal distribution of chromosomes and imbalanced chromosome segregation with lagging chromosome, loss of midbody and cytodieresis (Figure 4I–K). A dramatic increase in the number of apoptotic nuclei was also observed (Figure 4H, I) likely due to the mitotic catastrophe triggered by KAP1 loss.

The precise timing of G2/M genes expression during cell cycle is guaranteed by the BMYB/FOXM1-MuvB complex that assembles during the late S phase, binding to a common sequence in the G2/M genes known as cell cycle gene homology region (CHR) (37,38). Noticeably, 57.3% (n = 43) (Figure 4L) of the mitosis associated KAP1 target genes (Figure 4A) displayed CHR motif in their promoter, including the same BMYB and FOXM1. Indeed, siRNA-mediated KD of BMYB and FOXM1 restrains MPM cell

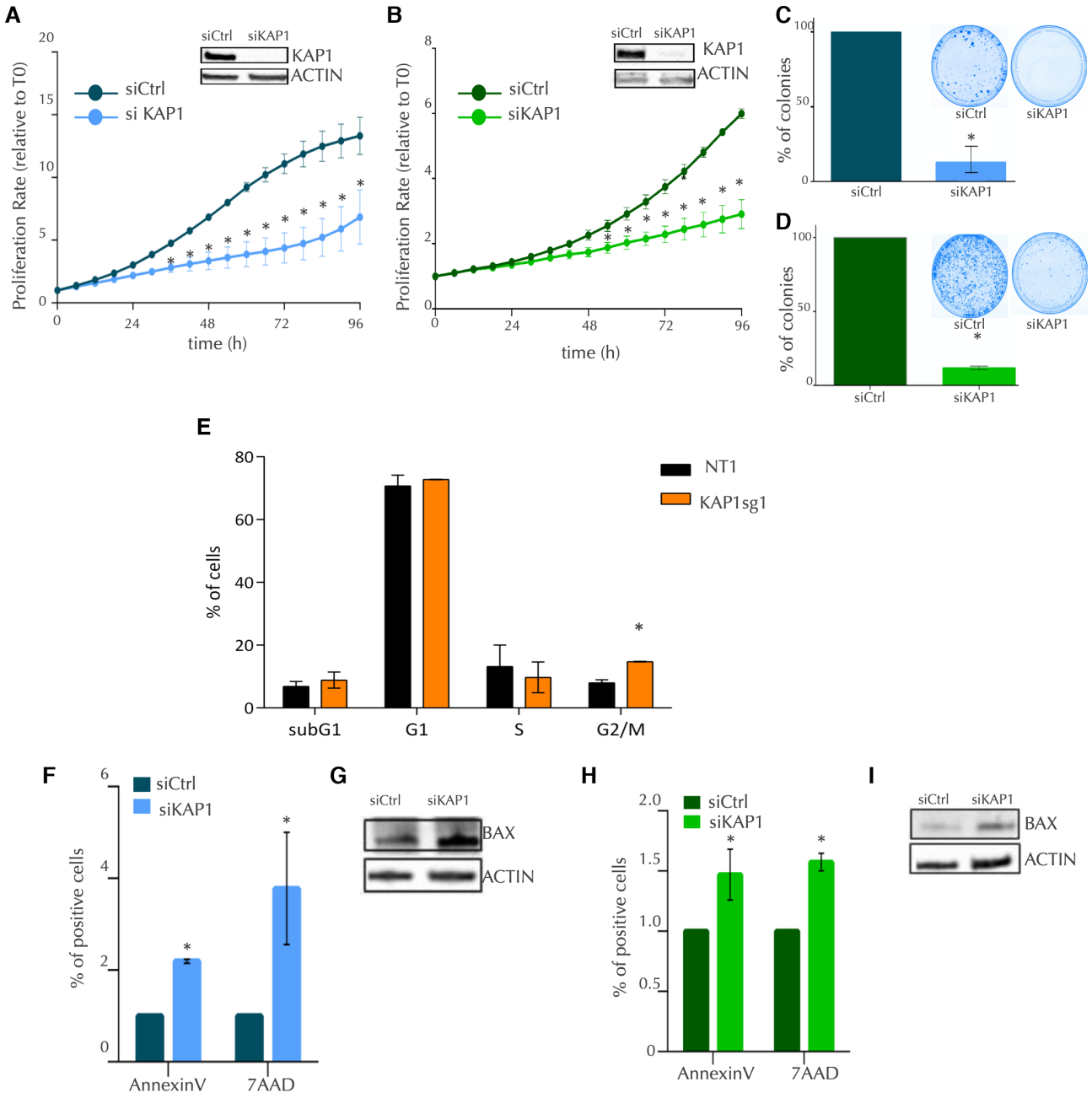

Figure 3. KAP1 inactivation strongly impairs proliferation of MPM cells and delays cell cycle. (**A**, **B**) Proliferation assays in MSTO-211H (A) and NCI-H2052 (B) cells reported as proliferation rate relative to day 0, measured with Incucyte S3 Live Cell Analysis (Sartorius). Data are represented as mean ± SEM; *$P < 0.05$; $N = 3$. The panels on top represent western blot of KAP1 protein loss upon KAP1 KD at 72 h after siRNA release. (**C**, **D**) KAP1 KD effect on colony forming ability of MSTO-211H (C) and NCI-H2052 (D) cells. Data are mean ± SEM; *$P < 0.05$; $N = 2$. (**E**) Cell cycle analysis of MSTO-211H/Cas9 NT1 versus KAP1-sg.1 cells performed with a FACS Canto cytometer upon Nicoletti staining. The analysis was performed 4 days after infection. Data are represented as mean ± SEM; *$P < 0.05$; $N = 3$. (**H**) Apoptosis analysis through Annexin V and 7AAD staining in MSTO-211H (F) and NCI-H2052 (H) cells. Cells were collected 72 h after transfection and analyzed with a FACS Canto cytometer. Data are represented as mean ± SEM; *$P < 0.05$; $N = 3$. (**G**, **I**) Western Blot of MPM cells showing accumulation of the pro-apoptotic protein BAX in KAP1 KD cells in MSTO-211H (G) and NCI-H2052 (I) cells at 72 h post transfection.

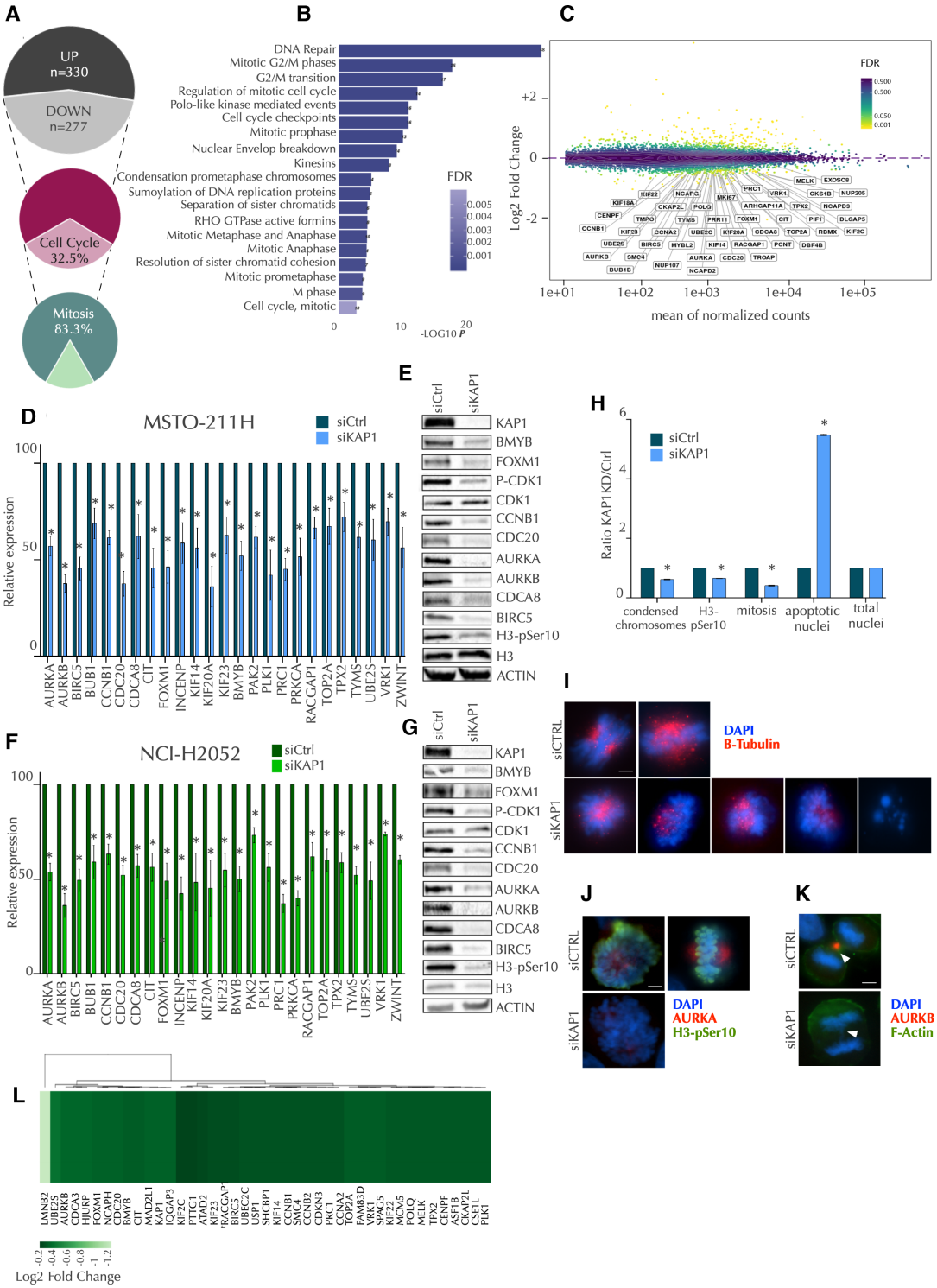

Figure 4. KAP1 KD results in down-regulation of G2/M genes. (**A**) Distribution of KAP1 target genes as emerged by RNA-seq profiling percentages of cell cycle and mitotic downregulated genes. (**B**) Barplot of the most significant enriched pathways (FDR<0.05) for genes that are downregulated from RNA-seq. (**C**) MA plot visualization of differential expression analysis performed on RNA-seq data. The essential core of downregulated genes is highlighted. (**D**–**G**) qRT-PCR and western blot validation of the indicated KAP1 target genes in siKAP1 and siCTRL cells in MSTO-211H (D, E) and NCI-H2052 cells (F, G). Data are represented as mean ± SEM; $*P < 0.05$; $N = 4$. (**H**) Distribution of mitotic morphological features in siKAP1 versus siCtrl MSTO-211H cells analyzed by immunofluorescence staining. (**I**) Immunofluorescence showing B-tubulin (red) in MSTO-211H siCTRL and siKAP1 cells. B-tubulin antibodies were used to visualize mitotic spindles. (**J**) Immunofluorescence staining of AURKA and H3-pSer10 in siKAP1 and siCtrl MSTO-211H cells. (**K**) Immunofluorescence staining of AURKB and F-actin in siKAP1 and siCtrl MSTO-211H cells. Scale bars 100 μm. (**L**) Heatmap of the 43 CHR genes that were significantly downregulated in KAP1 KO cells and showed KAP1 binding in their promoter by ChIP-seq analysis. Genes were grouped based on unsupervised hierarchical clustering according to expression values expressed as Log_2 Fold Change. The list of CHR genes was taken from Fischer *et al.* (38).

proliferation and severely reduced the expression of G2/M genes, partially (FOXM1) or completely (BMYB) mimicking the KAP1 KD effects (Supplementary Figure 7A–F) and suggesting that the inhibitory growth capacity of KAP1 KD MPM cells goes through the impairment of the transcriptional circuit that support G2/M execution. Noticeably, FOXM1, as a target of YAP/TAZ, has already been reported to be a dependency for MPM cells by Mizuno *et al.* (39).

CDK9 inhibitors impaired KAP1-dependent transcriptional program leading to MPM cell death

As activator of transcription, KAP1 has been shown to cooperate with context specific TFs and CDK9 to recruit and activate RNA-PolII on target genes promoter (19).

Indeed, analysis of KAP1 ChIP-seq tracks (40) showed that KAP1 binds at the Transcriptional Starting Site (TSS) of mitotic genes in correspondence of binding sites of active markers of transcription pSer2-RNA-PolII and CDK9 (Figure 5A). KAP1-ChIP on MSTO-211H cells confirmed that this factor binds to mitotic genes TSS region also in MPM (Figure 5B).

Co-IP experiments in MSTO-211H cells confirmed previously published data (19) that KAP1 interacts with CDK9 and both pSer2 and pSer5 RNA-PolII also in MPM (Figure 5C, D, Supplementary Figure 7G).

To take further these observations, we explored the effects of KAP1 KD on the assembly of the transcriptional complex on mitotic gene promoters. Coherently with the hypothesis that KAP1 is required for proficient RNA-PolII recruitment and activation, KAP1 KD resulted in a dramatic and specific displacement of RNA-PolII from the promoters of a subset of mitosis-associated KAP1 target genes, not observed for CD69 used as negative control (Figure 5F, Supplementary Figure 8A–C) (19) and a massive decrease of pSer2_RNA-PolII levels along the AURKB gene body (Figure 5G). As well, KAP1 KD determined a significant reduction of CDK9 and FOXM1 binding on the same promoters (Supplementary Figure 8D, E). To consolidate these data, we investigated the interaction of KAP1 with FOXM1 and RBBP4. Both these proteins are part of the active form of the MuvB complex that assembles on G2/M genes during S phase to turn on the mitotic gene program. Noticeably, we observed that KAP1 interacts with both FOXM1 and RBBP4 in MSTO-211H cells in Co-IP experiments (Figure 5C, E).

Next, we explored the possibility of pharmacologically targeting KAP1 function in MPM by abolishing its transcriptional cooperation with CDK9. Thus, MPM cell lines were treated with the Pan-CDK inhibitor AT7519 (41) or with the CDK9 specific inhibitor AZD4573 (42). Both drugs showed a dramatic effect on cell survival in both cell lines. AZD4573 was massively toxic for these cells at very low concentrations (MSTO-211H_EC50 = 23 nM; NCI-H2052_EC50 = 22.9 nM) (Supplementary Figure 8F, G) and it showed a dramatic dose-dependent cell growth inhibition in both cell models tested (Figure 5H, I). This was accompanied by the inability of the cells to actively entering mitosis with consequential increase of cell death (Figure 5J, K). Analysis of KAP1 target genes showed that AZD4573 significantly affected their expression mimicking KAP1-loss and suggesting that the lethal effects of these drugs in MPM acts primarily through the inhibition of KAP1 gene program (Figure 5L, M).

Model validation in a separate cohort of MPM patients

To validate these data *in vivo,* we analyzed two different MPM patients' datasets: 86 patients from the MPM-TCGA project and a retrospective cohort of 97 consecutive MPMs that underwent surgical resection in our Institution in the past 10 years (MPM-RE). Flow-chart of the analyses is provided in Figure 6A. For the MPM-TCGA dataset, 15 patients were removed because of lack of follow up and 71 had expression profile eligible for the analysis. In the MPM-RE cohort, the expression of KAP1 and its G2/M target genes was investigated by digital profiling using a custom panel (Supplementary Table 3). After quality check controls and data normalization, 86 RNA samples provided gene expression profile (GEP) eligible for further analyses (Figure 6A). Clinical data of these patients are provided in Table 1. Principal component analysis (PCA) showed that the expression of KAP1 and its targets strongly separated long- from short- term survivors (long-OS and short-OS) in both patient cohorts (Figure 6B, C). In line with our *in vitro* observations, KAP1 showed a significant positive correlation with all the target genes investigated in MPM patients in both groups (Figure 6D, E, Supplementary Figure 9A–D). Next, we explored the association of these genes with clinical aggressiveness evaluating their expression according to patients' overall survival (OS). Noticeably, the expression of KAP1 and of the majority of its targets was significantly higher in short-OS as compared with long-OS both in the MPM-TCGA (Figure 6F) and MPM-RE dataset (Figure 6G), confirming their association with aggressiveness of MPM. Coherently, survival analysis demonstrated a significant association with reduced survival probability (Figure 6H, I). In particular, 97.3% and 86.5% of the investigated genes showed negative prognostic value in the MPM-TCGA and MPM-RE dataset, respectively. KAP1 was confirmed as associated with reduced survival in both cohorts. Also, we took advantage of the MPM-RE cohort to evaluate the association of the remaining 17 essential genes identified by the genome-wide CRISPR/Cas9 screening with patients' survival. All these genes showed higher expression in high versus low OS, and 11 out of 17 genes were confirmed as significantly associated with reduced survival probability (Supplementary Figure 10A, B), therefore supporting the validity of our screening. Overall, these data confirmed *in vivo* that KAP1 and its associated gene program are important determinants of MPM clinical aggressiveness and underlined their potential as prognostic markers in the clinical management of MPM patients.

DISCUSSION

Nowadays, MPM represents a major clinical challenge. Being associated with asbestos exposure, its incidence is steadily increasing in many industrialized countries and it will soon become a relevant issue in many developing areas where the use of this silicate derivate is still largely diffuse (1–3).

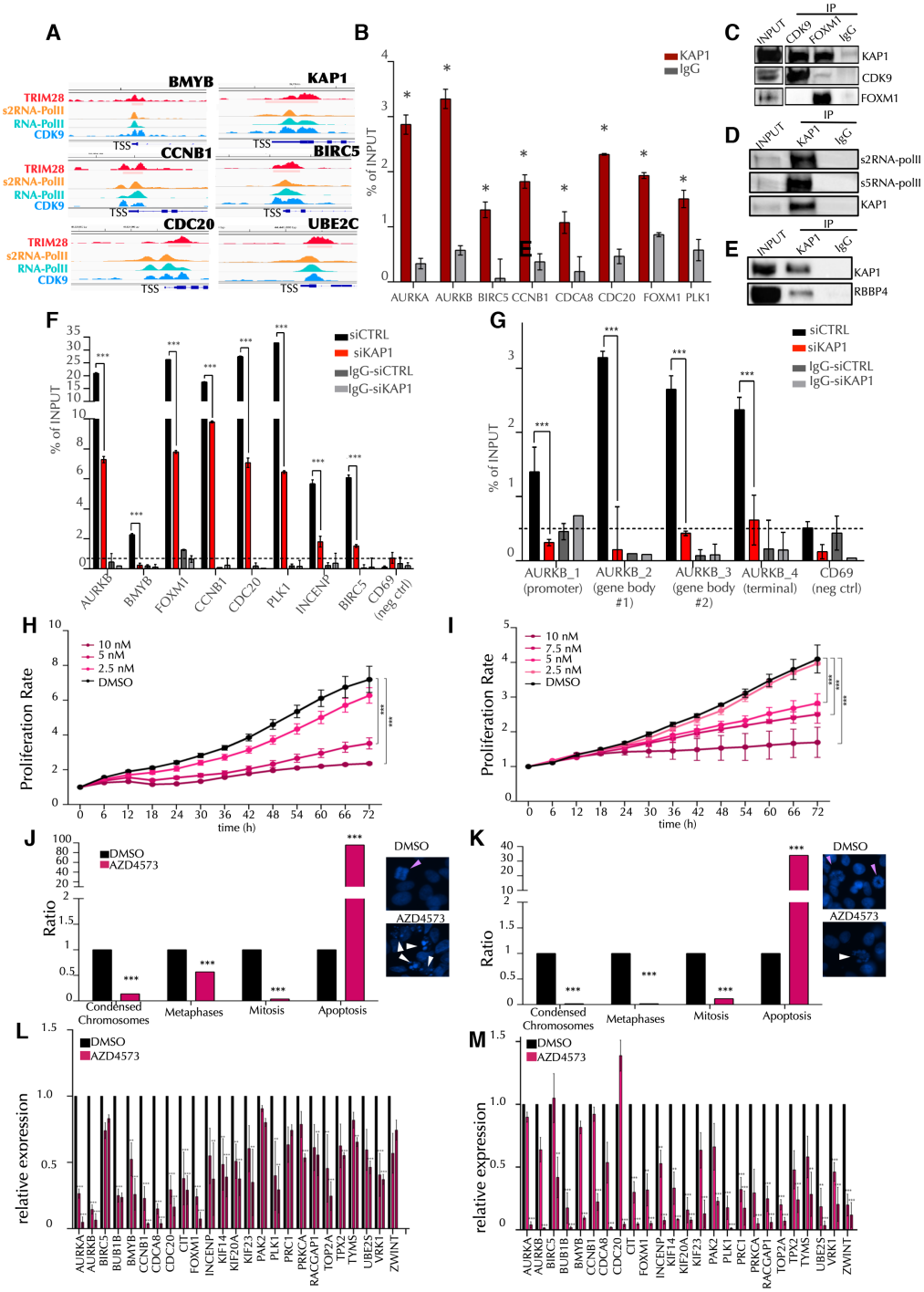

Figure 5. CDK9i phenocopied KAP1 loss, leading to dose-dependent MPM cell growth inhibition. (**A**) Visualization of KAP1, CDK9, RNA-PolII and pSer2-RNA-PolII binding profiles on selected target genes with Integrative Genome Viewer (IGV). (**B**) ChIP analysis of KAP1 binding on its mitotic target genes. Values are represented as percentage of input. Data are expressed as mean + SD and one representative experiment is reported. (**C**–**E**) Co-IP experiments in MSTO-211H cells. IP and WB were conducted with the indicated antibodies. One representative experiment is reported; $N = 3$. (**F**) ChIP analysis of RNA-PolII binding on KAP1 mitotic target gene promoters in siCTRL and siKAP1 MSTO-211H cells; (CD69 negative control). Values are represented as percentage of input. Data are expressed as mean ± SD and one representative experiment is reported. (**G**) ChIP analysis showing pSer2-RNA-PolII binding alongside the gene-body of AURKB in siCTRL and siKAP1 MSTO-211H cells; CD69 promoter is used as a negative control. Values are represented as percentage of input. Data are expressed as mean ± SD and one representative experiment is reported. (**H**, **I**) Proliferation assays showing the effect of the CDK9i AZD4573 at sublethal doses in MSTO-211H (H) and NCI-H2052 (I) cell lines. Proliferation rates were measured with Incucyte S3 Live Cell Analysis (Sartorius). Data are expressed as mean ± SEM; $*P < 0.05$, $**P < 0.01$, $***P < 0.001$; $N = 3$. (J, K) Distribution of mitotic morphological features in 10 nM AZD4573 versus DMSO treated MSTO-211H (**J**) and NCI-H2052 (**K**) cells analyzed by immunofluorescence staining. Inserts display representative immunofluorescence showing DAPI staining in 10 nM AZD4573 versus DMSO treated MSTO-211H and NCI-H2052 cells. Pink arrows indicate mitotic nuclei while white arrows indicate apoptotic nuclei. (**L**, **M**) qRT-PCR analysis of a subset of KAP1 direct target genes in MPM cell lines treated with DMSO or sublethal doses of AZD4573. Data are expressed as mean ± SEM. $*P < 0.05$, $**P < 0.01$, $***P < 0.001$.

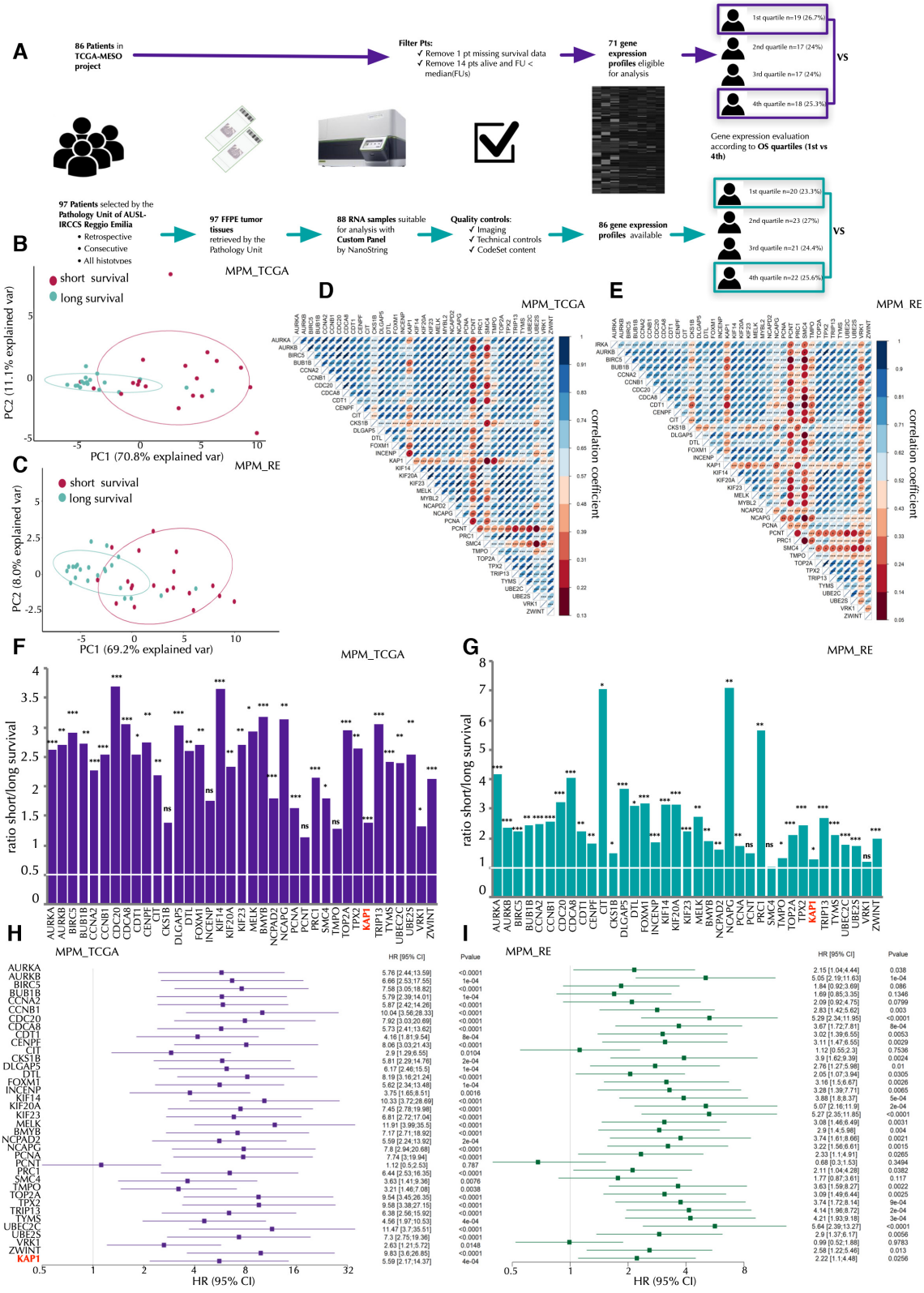

Figure 6. KAP1 and its dependent gene program are prognostic marker in MPM patients. (**A**) Flowchart of the validation analysis in the MPM-TCGA and MPM-RE cohort. FU: follow up. (**B**, **C**) PCA analysis of the distribution of long and short survivors (I and IV quartile) based on the expression of KAP1 and its targets genes in both cohorts (FDR < 0.05). (**D**, **E**) Expression correlation matrix (Spearman test) within KAP1 and its mitotic target genes in the MPM-TCGA (D) and MPM-RE (E) cohorts; $*P < 0.05$, $**P < 0.01$, $***P < 0.001$. (F, G) Histogram representing the ratio of expression of the indicated genes in short versus long survivors (I and IV quartile). $*P < 0.05$, $**P < 0.01$, $***P < 0.001$ MPM-TCGA (**F**) and MPM-RE (**G**) datasets. (**H**, **I**) Forest-Plot displaying the correlation of KAP1 and its target genes with reduced survival probability in MPM patients. The analysis in the MPM-RE cohort (I) was corrected for surgery and chemotherapy treatment.

Lack of markers for the early detection and limitations of currently available therapeutic options are the reasons of the massive mortality rate that characterizes this disease. These shortcomings are the spontaneous consequence of the still poorly characterized biology of these tumors. Indeed, despite the relevant amount of information provided by the recent omics studies in MPM, the events marking genesis and evolution of this disease remain elusive and difficult to be used for the development of new therapeutic opportunities.

Mutational profiling showed that differently from other types of cancer, MPM is associated primarily to loss of function of tumor suppressor genes and phylogenetic tree topology reveals extensive inter-patient and intra-patient heterogeneity failing to define evolutionary constrains that could represent potential vulnerabilities (7,8,43,44).

Net of this complex biological framework, the therapeutic options for MPM patients are still limited to surgery, standard regimens of chemotherapy and more recently immunotherapy (5,45).

Taking a different perspective, here we employed a functional approach combined with patients' omics and clinical data with the idea that perturbing the function of single genes and monitoring the consequential effects could provide information on new non-genetic vulnerabilities of MPMs, overcoming the limitations of purely descriptive profiling strategies. Indeed, we discovered a core of functionally related MPM essential genes whose perturbation impairs cell viability and whose expression in patients underlines aggressive disease and reduced survival probability. Not surprisingly, our data identified processes converging on chromatin organization and function as fundamental for the maintenance and progression of MPM cells. This is in line with the consolidating hypothesis that alterations in the epigenome are indeed major drivers of the asbestos-induced carcinogenetic process in this disease and with the evidence that major genetic alterations in MPM hit on chromatin regulators like BAP1, TP53, SETD2 and SETDB1 (5,7,8,12,46,47).

Among the core of 18 essential genes that were identified in our analysis, we focused on KAP1 which expression profoundly marked the distinction between long and short survivors in MPM patients associating with an ominous outcome.

KAP1 (also known as TRIM28) is a multifunctional chromatin reader that works either as structural or functional element within multiprotein complexes catalyzing both positive and negative transcriptional regulation (14,15,18,19,48–50). Consistent with its pivotal role in chromatin functions, KAP1 has been described as overexpressed in different types of cancer and preferentially but not exclusively associated with aggressiveness and poor prognosis. Mechanistically, KAP1 has been linked to many different biological processes, including silencing of oncosuppressors, DNA damage response, epithelial to mesenchymal transition and pluripotency regulation (14). Still, *in virtue* of such complexity, KAP1 molecular function in cancer remains elusive. Likely, its polyhedric functions are differentially declined according to cell-specific and time-specific cancer needs. According to the DEPMAP data, the dependency from KAP1 is not restricted to MPM, since cell lines from different tumor settings showed to rely on this factor for survival (Supplementary Figure S4A). We used publicly available datasets to define the existence of a common genetic signature that could explain the dependency from KAP1 both across cancer and within the MPM dataset, but we were not able to define any significant correlation. As such we cannot exclude that KAP1 may be a vulnerability only in specific subsets of MPM patients. Indeed, even if we did not observe significant correlation with the BAP1 mutation in the DEPMAP MPM cell lines dataset we acknowledge as a limitation of this study the fact that all the experiments were conducted in two cell lines that are not BAP1 mutated.

In the specific context of MPM, we discovered a previously unknown and unexpected function of KAP1 in cell cycle regulation. In absence of KAP1, MPM cells are impaired in carrying on mitosis dying in consequence of the prolonged block, explaining the essentiality of this factor for MPM cells' expansion.

Acting as transcriptional activator, KAP1 is required for proficient G2/M transition and mitosis execution, being responsible for the expression of a core of genes governing this peculiar phase of the cell cycle. We demonstrated for the first time that KAP1 binds to G2/M gene promoters at the level of TSS and the CHR motif, in correspondence of CDK9 and RNA-PolII binding sites. We showed that KAP1 interacts, together with CDK9 and RNA-PolII with the MuvB complex in its transcriptionally active form. We report that, in absence of KAP1 the RNA-PolII is dislocated from the G2/M gene promoters and its actively elongating form (pSer2-RNA-PolII) reduced along the gene body. Consequentially, the expression of major mitotic players including AURKA and AURKB is dramatically reduced in absence of KAP1 producing massive consequences on chromosome condensation, alignment and segregation. At last, in absence of KAP1, MPM cells are unable to carry on mitosis dying in consequence of the prolonged block, explaining essentiality of this factor for MPM cells' expansion (graphical abstract).

In accordance with its dual function in transcription, our gene expression profiling data showed that KAP1 KO lead to a comparable number of upregulated and downregulated genes. The overall $\log_2$ fold change for both list of genes was quite low, consistently with previous evidence reporting small effects of KAP1 loss on the human transcriptome (51). In spite of this, our experiments demonstrated that the transcriptional effect of KAP1 KD is biologically relevant. We hypothesize that KAP1 acts not just as a trigger of specific genes, but as a coordinator of entire gene programs that sustain specific biological functions. As such, the simultaneous perturbation of the entire program by KAP1 KD results in a biological relevant effect even if the single genes are only modestly affected.

Cancer evolution requires rapid and efficient adaptation of the transcriptional programs in response to multiple cell-intrinsic and extrinsic stimuli (52). Precise regulation of RNA-PolII activity including recruitment, pausing and pause release on specific genes guarantee this plasticity and the functional efficiency of cancer cells (53,54).

Bacon et al. recently showed that in the landscape of RNA-PolII controllers, KAP1 plays a very unique function being able to control and integrate both steps of RNA-PolII cycle: initiation and elongation. As suggested by the Authors, this KAP1-centered mechanism is commonly used by cancer cells to time the activation of cancer supportive pathways and activate transcriptional programs in response to specific conditions (19). Our data fit coherently within this model.

In the ability of KAP1 to prime RNA-PolII into active elongation, CDK9 has been shown to play a pivotal role. For its centrality into the dynamics of gene expression, CDK9 has been regarded as a promising target for new anticancer drugs. Indeed, several inhibitors have been developed and tested in a variety of hematological cancers and solid tumors in preclinical and clinical settings (19,52–56).

We hypothesized that hitting KAP1 function through the inhibition of its functional partner CDK9 could represent a possible therapeutic strategy in MPM. Indeed, we showed that both pan-CDKi and specific CDK9i are dramatically lethal for MPM cells even at very low concentrations. Even if very preliminary, this evidence lay the basis for the employment of these compounds in the clinical management of MPMs, setting an example of how functional screening may result more effective than purely descriptive omics profiling in the definition of new therapies in orphan diseases.

One of the major strengths of our analysis is the integration of functional data with patients profiling and clinical information. We used data from the MPM dataset of TCGA to filter gene candidates from the functional screening pointing on factors associated with disease aggressiveness in real life. Then we used an independent cohort of patients to validate our observations and the developed model, linking basic biology to clinical application.

Even if several valuable biomolecular tools (57,58) to improve risk-based stratification of MPM-patients have been recently described, our results identify KAP1 and its target genes candidate to become potential tools in the prognostication of disease aggressiveness helping clinicians to tailor patients' management according to real needs.

In conclusion, through an integrated approach we discovered KAP1 as a new non-genetic vulnerability in MPM, showing that its centrality in this setting is linked to a previously unknown function of this factor in setting the timing of G2/M gene expression. These data not only represent a significant advance in the knowledge of the molecular basis of MPM, but provide a solid proof of principle for the development of new prognostic tools and for the introduction of new drugs in the management of this disease.

DATA AVAILABILITY

RNA-sequencing data are available at ArrayExpress (E-MTAB-10942). Nanostring gene expression data are available at GEO repository (accession number: GSE183088)

SUPPLEMENTARY DATA

Supplementary Data are available at NAR Cancer Online.

ACKNOWLEDGEMENTS

We wish to thank Marina Grassi for technical support and all the members of the lab for stimulating discussion

FUNDING

Bando per la valorizzazione della Ricerca Istituzionale in ambito oncologico 2020 (5permille); Italian Ministry of Health – Ricerca Corrente Annual Program 2022; Eugenia Lorenzini was supported by AIRC fellowship for Italy.

Conflict of interest statement. The authors declare that they have no competing interests

REFERENCES

1. Galateau-Salle,F., Churg,A., Roggli,V., Travis,W.D. and World Health Organization Committee for Tumors of the PleuraWorld Health Organization Committee for Tumors of the Pleura (2016) The 2015 World Health Organization classification of tumors of the pleura: advances since the 2004 classification. *J. Thorac. Oncol.*, **11**, 142–154.
2. Carbone,M., Ly,B.H., Dodson,R.F., Pagano,I., Morris,P.T., Dogan,U.A., Gazdar,A.F., Pass,H.I. and Yang,H. (2012) Malignant mesothelioma: facts, myths, and hypotheses. *J. Cell. Physiol.*, **227**, 44–58.
3. Bianchi,C. and Bianchi,T. (2007) Malignant mesothelioma: global incidence and relationship with asbestos. *Ind. Health*, **45**, 379–387.
4. Lococo,F., Torricelli,F., Lang-Lazdunski,L., Veronesi,G., Rena,O., Paci,M., Casadio,C., Piana,S., Novellis,P., Di Stefano,T.S. *et al.* (2020) Survival results in biphasic malignant pleural mesothelioma patients: a multicentric analysis. *J. Thorac. Cardiovasc. Surg.*, **159**, 1584–1593.
5. Yap,T.A., Aerts,J.G., Popat,S. and Fennell,D.A. (2017) Novel insights into mesothelioma biology and implications for therapy. *Nat. Rev. Cancer*, **17**, 475–488.
6. Bueno,R., Stawiski,E.W., Goldstein,L.D., Durinck,S., De Rienzo,A., Modrusan,Z., Gnad,F., Nguyen,T.T., Jaiswal,B.S., Chirieac,L.R. *et al.* (2016) Comprehensive genomic analysis of malignant pleural mesothelioma identifies recurrent mutations, gene fusions and splicing alterations. *Nat. Genet.*, **48**, 407–416.
7. Hmeljak,J., Sanchez-Vega,F., Hoadley,K.A., Shih,J., Stewart,C., Heiman,D., Tarpey,P., Danilova,L., Drill,E., Gibb,E.A. *et al.* (2018) Integrative molecular characterization of malignant pleural mesothelioma. *Cancer Discov.*, **8**, 1548–1565.
8. Hylebos,M., Van Camp,G., van Meerbeeck,J.P. and Op de Beeck,K. (2016) The genetic landscape of malignant pleural mesothelioma: results from massively parallel sequencing. *J. Thorac. Oncol.*, **11**, 1615–1626.
9. Guo,G., Chmielecki,J., Goparaju,C., Heguy,A., Dolgalev,I., Carbone,M., Seepo,S., Meyerson,M. and Pass,H.I. (2015) Whole-exome sequencing reveals frequent genetic alterations in BAP1, NF2, CDKN2A, and CUL1 in malignant pleural mesothelioma. *Cancer Res.*, **75**, 264–269.
10. Kato,S., Tomson,B.N., Buys,T.P.H., Elkin,S.K., Carter,J.L. and Kurzrock,R. (2016) Genomic landscape of malignant mesotheliomas. *Mol. Cancer Ther.*, **15**, 2498–2507.
11. Christensen,B.C., Godleski,J.J., Marsit,C.J., Houseman,E.A., Lopez-Fagundo,C.Y., Longacker,J.L., Bueno,R., Sugarbaker,D.J., Nelson,H.H. and Kelsey,K.T. (2008) Asbestos exposure predicts cell cycle control gene promoter methylation in pleural mesothelioma. *Carcinogenesis*, **29**, 1555–1559.
12. Goto,Y., Shinjo,K., Kondo,Y., Shen,L., Toyota,M., Suzuki,H., Gao,W., An,B., Fujii,M., Murakami,H. *et al.* (2009) Epigenetic profiles distinguish malignant pleural mesothelioma from lung adenocarcinoma. *Cancer Res.*, **69**, 9073–9082.
13. Mohammad,H.P., Barbash,O. and Creasy,C.L. (2019) Targeting epigenetic modifications in cancer therapy: erasing the roadmap to cancer. *Nat. Med.*, **25**, 403–418.
14. Czerwińska,P., Mazurek,S. and Wiznerowicz,M. (2017) The complexity of TRIM28 contribution to cancer. *J. Biomed. Sci.*, **24**, 63.

15. Iyengar,S. and Farnham,P.J. (2011) KAP1 protein: an enigmatic master regulator of the genome. *J. Biol. Chem.*, **286**, 26267–26276.
16. Schultz,D.C., Ayyanathan,K., Negorev,D., Maul,G.G. and Rauscher,F.J. (2002) SETDB1: a novel KAP-1-associated histone H3, lysine 9-specific methyltransferase that contributes to HP1-mediated silencing of euchromatic genes by KRAB zinc-finger proteins. *Genes Dev.*, **16**, 919–932.
17. Ivanov,A.V., Peng,H., Yurchenko,V., Yap,K.L., Negorev,D.G., Schultz,D.C., Psulkowski,E., Fredericks,W.J., White,D.E., Maul,G.G. *et al.* (2007) PHD domain-mediated E3 ligase activity directs intramolecular sumoylation of an adjacent bromodomain required for gene silencing. *Mol. Cell*, **28**, 823–837.
18. McNamara,R.P., Reeder,J.E., McMillan,E.A., Bacon,C.W., McCann,J.L. and D'Orso,I. (2016) KAP1 recruitment of the 7SK snRNP complex to promoters enables transcription elongation by RNA polymerase II. *Mol. Cell*, **61**, 39–53.
19. Bacon,C.W., Challa,A., Hyder,U., Shukla,A., Borkar,A.N., Bayo,J., Liu,J., Wu,S.-Y., Chiang,C.-M., Kutateladze,T.G. *et al.* (2020) KAP1 is a chromatin reader that couples steps of RNA polymerase II transcription to sustain oncogenic programs. *Mol. Cell*, **78**, 1133–1151.
20. Sanjana,N.E., Shalem,O. and Zhang,F. (2014) Improved vectors and genome-wide libraries for CRISPR screening. *Nat. Methods*, **11**, 783–784.
21. Gobbi,G., Donati,B., Do Valle,I.F., Reggiani,F., Torricelli,F., Remondini,D., Castellani,G., Ambrosetti,D.C., Ciarrocchi,A. and Sancisi,V. (2019) The Hippo pathway modulates resistance to BET proteins inhibitors in lung cancer cells. *Oncogene*, **38**, 6801–6817.
22. Reggiani,F., Sauta,E., Torricelli,F., Zanetti,E., Tagliavini,E., Santandrea,G., Gobbi,G., Damia,G., Bellazzi,R., Ambrosetti,D. *et al.* (2021) An integrative functional genomics approach reveals EGLN1 as a novel therapeutic target in KRAS mutated lung adenocarcinoma. *Mol. Cancer*, **20**, 63.
23. Tsherniak,A., Vazquez,F., Montgomery,P.G., Weir,B.A., Kryukov,G., Cowley,G.S., Gill,S., Harrington,W.F., Pantel,S., Krill-Burger,J.M. *et al.* (2017) Defining a cancer dependency map. *Cell*, **170**, 564–576.
24. Rossi,T., Pistoni,M., Sancisi,V., Gobbi,G., Torricelli,F., Donati,B., Ribisi,S., Gugnoni,M. and Ciarrocchi,A. (2020) RAIN is a novel enhancer-associated lncRNA that controls RUNX2 expression and promotes breast and thyroid cancer. *Mol. Cancer Res.*, **18**, 140–152.
25. Gugnoni,M., Manicardi,V., Torricelli,F., Sauta,E., Bellazzi,R., Manzotti,G., Vitale,E., de Biase,D., Piana,S. and Ciarrocchi,A. (2021) Linc00941 is a novel transforming growth factor β target that primes papillary thyroid cancer metastatic behavior by regulating the expression of cadherin 6. *Thyroid*, **31**, 247–263.
26. Ciarrocchi,A., D'Angelo,R., Cordiglieri,C., Rispoli,A., Santi,S., Riccio,M., Carone,S., Mancia,A.L., Paci,S., Cipollini,E. *et al.* (2009) Tollip is a mediator of protein sumoylation. *PLoS One*, **4**, e4404.
27. Riccardi,C. and Nicoletti,I. (2006) Analysis of apoptosis by propidium iodide staining and flow cytometry. *Nat. Protoc.*, **1**, 1458–1461.
28. Dobin,A., Davis,C.A., Schlesinger,F., Drenkow,J., Zaleski,C., Jha,S., Batut,P., Chaisson,M. and Gingeras,T.R. (2013) STAR: ultrafast universal RNA-seq aligner. *Bioinformatics*, **29**, 15–21.
29. Li,B. and Dewey,C.N. (2011) RSEM: accurate transcript quantification from RNA-Seq data with or without a reference genome. *BMC Bioinf.*, **12**, 323.
30. Love,M.I., Huber,W. and Anders,S. (2014) Moderated estimation of fold change and dispersion for RNA-seq data with DESeq2. *Genome Biol.*, **15**, 550.
31. Kuleshov,M.V., Jones,M.R., Rouillard,A.D., Fernandez,N.F., Duan,Q., Wang,Z., Koplev,S., Jenkins,S.L., Jagodnik,K.M., Lachmann,A. *et al.* (2016) Enrichr: a comprehensive gene set enrichment analysis web server 2016 update. *Nucleic Acids Res.*, **44**, W90–W97.
32. Bindea,G., Mlecnik,B., Hackl,H., Charoentong,P., Tosolini,M., Kirilovsky,A., Fridman,W.-H., Pagès,F., Trajanoski,Z. and Galon,J. (2009) ClueGO: a Cytoscape plug-in to decipher functionally grouped gene ontology and pathway annotation networks. *Bioinformatics*, **25**, 1091–1093.
33. Luminari,S., Donati,B., Casali,M., Valli,R., Santi,R., Puccini,B., Kovalchuk,S., Ruffini,A., Fama,A., Berti,V. *et al.* (2020) A gene expression-based model to predict metabolic response after two courses of ABVD in Hodgkin lymphoma patients. *Clin. Cancer Res.*, **26**, 373–383.
34. Krasinskas,A.M., Bartlett,D.L., Cieply,K. and Dacic,S. (2010) CDKN2A and MTAP deletions in peritoneal mesotheliomas are correlated with loss of p16 protein expression and poor survival. *Mod. Pathol.*, **23**, 531–538.
35. Tie,C.H., Fernandes,L., Conde,L., Robbez-Masson,L., Sumner,R.P., Peacock,T., Rodriguez-Plata,M.T., Mickute,G., Gifford,R., Towers,G.J. *et al.* (2018) KAP1 regulates endogenous retroviruses in adult human cells and contributes to innate immune control. *EMBO Rep.*, **19**, e45000.
36. Joukov,V. and De Nicolo,A. (2018) Aurora-PLK1 cascades as key signaling modules in the regulation of mitosis. *Sci. Signal*, **11**, eaar4195.
37. Müller,G.A., Quaas,M., Schümann,M., Krause,E., Padi,M., Fischer,M., Litovchick,L., DeCaprio,J.A. and Engeland,K. (2012) The CHR promoter element controls cell cycle-dependent gene transcription and binds the DREAM and MMB complexes. *Nucleic Acids Res.*, **40**, 1561–1578.
38. Fischer,M., Quaas,M., Steiner,L. and Engeland,K. (2016) The p53-p21-DREAM-CDE/CHR pathway regulates G2/M cell cycle genes. *Nucleic Acids Res.*, **44**, 164–174.
39. Mizuno,T., Murakami,H., Fujii,M., Ishiguro,F., Tanaka,I., Kondo,Y., Akatsuka,S., Toyokuni,S., Yokoi,K., Osada,H. *et al.* (2012) YAP induces malignant mesothelioma cell proliferation by upregulating transcription of cell cycle-promoting genes. *Oncogene*, **31**, 5117–5122.
40. McNamara,R.P., Guzman,C., Reeder,J.E. and D'Orso,I. (2016) Genome-wide analysis of KAP1, the 7SK snRNP complex, and RNA polymerase II. *Genom Data*, **7**, 250–255.
41. Santo,L., Vallet,S., Hideshima,T., Cirstea,D., Ikeda,H., Pozzi,S., Patel,K., Okawa,Y., Gorgun,G., Perrone,G. *et al.* (2010) AT7519, A novel small molecule multi-cyclin-dependent kinase inhibitor, induces apoptosis in multiple myeloma via GSK-3beta activation and RNA polymerase II inhibition. *Oncogene*, **29**, 2325–2336.
42. Cidado,J., Boiko,S., Proia,T., Ferguson,D., Criscione,S.W., San Martin,M., Pop-Damkov,P., Su,N., Roamio Franklin,V.N., Sekhar Reddy Chilamakuri,C. *et al.* (2020) AZD4573 is a highly selective CDK9 inhibitor that suppresses MCL-1 and induces apoptosis in hematologic cancer cells. *Clin. Cancer Res.*, **26**, 922–934.
43. Zhang,M., Luo,J.-L., Sun,Q., Harber,J., Dawson,A.G., Nakas,A., Busacca,S., Sharkey,A.J., Waller,D., Sheaff,M.T. *et al.* (2021) Clonal architecture in mesothelioma is prognostic and shapes the tumour microenvironment. *Nat. Commun.*, **12**, 1751.
44. Meiller,C., Montagne,F., Hirsch,T.Z., Caruso,S., de Wolf,J., Bayard,Q., Assié,J.-B., Meunier,L., Blum,Y., Quetel,L. *et al.* (2021) Multi-site tumor sampling highlights molecular intra-tumor heterogeneity in malignant pleural mesothelioma. *Genome Med*, **13**, 113.
45. Rijavec,E., Biello,F., Barletta,G., Dellepiane,C. and Genova,C. (2022) Novel approaches for the treatment of unresectable malignant pleural mesothelioma: a focus on immunotherapy and target therapy (Review). *Mol. Clin. Oncol.*, **16**, 89.
46. Lorenzini,E., Ciarrocchi,A. and Torricelli,F. (2021) Molecular fingerprints of malignant pleural mesothelioma: not just a matter of genetic alterations. *J. Clin. Med.*, **10**, 2470.
47. Sage,A.P., Martinez,V.D., Minatel,B.C., Pewarchuk,M.E., Marshall,E.A., MacAulay,G.M., Hubaux,R., Pearson,D.D., Goodarzi,A.A., Dellaire,G. *et al.* (2018) Genomics and epigenetics of malignant mesothelioma. *High Throughput*, **7**, E20.
48. Peng,H., Begg,G.E., Schultz,D.C., Friedman,J.R., Jensen,D.E., Speicher,D.W. and Rauscher,F.J. (2000) Reconstitution of the KRAB-KAP-1 repressor complex: a model system for defining the molecular anatomy of RING-B box-coiled-coil domain-mediated protein-protein interactions. *J. Mol. Biol.*, **295**, 1139–1162.
49. Li,M., Xu,X., Chang,C.-W. and Liu,Y. (2020) TRIM28 functions as the SUMO E3 ligase for PCNA in prevention of transcription induced DNA breaks. *Proc. Natl. Acad. Sci. U.S.A.*, **117**, 23588–23596.
50. Liang,Q., Deng,H., Li,X., Wu,X., Tang,Q., Chang,T.-H., Peng,H., Rauscher,F.J., Ozato,K. and Zhu,F. (2011) Tripartite motif-containing protein 28 is a small ubiquitin-related modifier E3 ligase and negative regulator of IFN regulatory factor 7. *J. Immunol.*, **187**, 4754–4763.

51. Iyengar,S., Ivanov,A.V., Jin,V.X., Rauscher,F.J. and Farnham,P.J. (2011) Functional analysis of KAP1 genomic recruitment. *Mol. Cell. Biol.*, **31**, 1833–1847.
52. Bradner,J.E., Hnisz,D. and Young,R.A. (2017) Transcriptional addiction in cancer. *Cell*, **168**, 629–643.
53. Muse,G.W., Gilchrist,D.A., Nechaev,S., Shah,R., Parker,J.S., Grissom,S.F., Zeitlinger,J. and Adelman,K. (2007) RNA polymerase is poised for activation across the genome. *Nat. Genet.*, **39**, 1507–1511.
54. Grünberg,S. and Hahn,S. (2013) Structural insights into transcription initiation by RNA polymerase II. *Trends Biochem. Sci*, **38**, 603–611.
55. Mandal,R., Becker,S. and Strebhardt,K. (2021) Targeting CDK9 for anti-cancer therapeutics. *Cancers (Basel)*, **13**, 2181.
56. Egloff,S. (2021) CDK9 keeps RNA polymerase II on track. *Cell. Mol. Life Sci.*, **78**, 5543–5567.
57. Bai,Y., Wang,X., Hou,J., Geng,L., Liang,X., Ruan,Z., Guo,H., Nan,K. and Jiang,L. (2020) Identification of a five-gene signature for predicting survival in malignant pleural mesothelioma patients. *Front Genet*, **11**, 899.
58. Blum,Y., Meiller,C., Quetel,L., Elarouci,N., Ayadi,M., Tashtanbaeva,D., Armenoult,L., Montagne,F., Tranchant,R., Renier,A. *et al.* (2019) Dissecting heterogeneity in malignant pleural mesothelioma through histo-molecular gradients for clinical applications. *Nat. Commun.*, **10**, 1333.